Optimizing the surface of manufactured components for friction, adhesion, and convective heat transfer

Henara L. Costa,* Francisco J. Profito, Xuan Zhang, and Karen Ann Thole

The manufacturing process defines not only the component's geometry, but also how its surface senses and interacts with the outside world via its topography. Every manufactured surface is rough, but the component can benefit from the roughness control. Topography in functional surfaces is optimized either by controlling the manufacturing parameters or by post-manufacturing surface patterning technologies. However, how are topographic features measured and characterized? How do rough surfaces contact each other? What happens if fluid is present at the contact interface? And what are the mechanisms that correlate surface topography and its functionalities? This article will cover the engineering of surface topography in manufacturing by addressing empirical advancements and scientific understanding in the field. The functionalities covered are adhesion, friction, and convective heat transfer. Relatively large surface structures used for heat transfer mainly take advantage of recent advances in additive manufacturing, while conventional manufacturing processes and deterministic surface patterning techniques are discussed for the control of adhesion and friction.

Introduction

Manufactured components are always rough, even when super-finishing techniques are employed.[1] The interaction of the component's surface with either mating surfaces or the surrounding media occurs via its surface topography. For contact with soft materials or fluids, the contact area is the contour of the rough topography and hence, larger than the apparent contact area; for two hard-material contacts, the true contact area is often thousands of times smaller as contact occurs only at the highest protrusions. Thus, the component´s surface properties are highly dependent on roughness.

Surface topography of a finished component ranges from randomly distributed asperities resulting from manufacturing to fairly repeatable patterns produced during post-machining processes and deterministic patterns specially engineered to meet the component's function. The literature often refers to such surfaces as functional, engineered, patterned, structured, or textured surfaces.[2] On the one hand, surface patterning, structuring, and texturing are synonyms that often explicitly refer to specially designed deterministic patterns, although, in the real world, no surface is perfectly deterministic as it will always have stochastic features. On the other hand, surface functionalization can also be achieved via the roughness obtained during manufacturing without additional finishing processes. Characterizing the surface topography of functional surfaces, especially those in the deterministic spectrum, is a complex issue, which cannot be fully described by conventional surface-characterization methods and metrics.[3]

The component's surface contacts a mating counterface in tribological contacts and adhesives. Although it has long been recognized that only the highest asperities come into real contact between stiff surfaces (much less so for compliant surfaces), analytical and numerical modeling of manufactured surfaces' contact still pose challenges in many tribological applications, particularly when lubricant is present at the interface. Other reviews in the literature[4] and in this issue address the contact mechanics of rough surfaces and mixed lubrication modeling in greater detail.

The surface topography can confer many functionalities to manufactured components; a full review on functionalities of patterned surfaces can be found in Reference 2. The topic has experienced intensive interest and research in the last

Henara L. Costa, School of Engineering, Federal University of Rio Grande, Rio Grande, Brazil; henaracosta@furg.br
Francisco J. Profito, Polytechnic School, University of São Paulo, São Paulo, Brazil; fprofito@usp.br
Xuan Zhang, INM-Leibniz Institute for New Materials, Saarbrücken, Germany; xuan.zhang@leibniz.inm.de
Karen Ann Thole, Department of Mechanical Engineering, The Pennsylvania State University, University Park, USA; kthole@psu.edu
*Corresponding author
doi:10.1557/s43577-022-00467-3

decades, particularly from an experimental perspective. However, the mechanisms underlying surface functionalities still need further understanding and consensus to design optimal surface patterns. In particular, this article will cover how, after decades of empirical advancements, recent work has leveraged scientific understanding to use advanced manufacturing and surface patterning to achieve optimal surface performance. First, recent advances in surface characterization of feature-based topography are presented, followed by a brief overview of the surface patterning technologies mostly used today; more extensive reviews on surface patterning technologies can be found in References 5 and 6. Then, the mechanisms involved in controlling adhesion, friction, and convective heat transfer in manufacturing components via surface topography are discussed. Finally, an examination of the state of the art in methods for modeling and simulation of adhesion and mixed lubrication of patterned surfaces is presented.

Topography characterization of functional surfaces

Engineering surfaces constitute the boundary of geometrical elements with their environment and are directly associated with the accuracy and precision of engineering components. Surface topography affects how surfaces interact with each other in dry and lubricated tribological applications and is relevant for wet adhesion and convective heat transfer. The surface topography characteristics are tightly related to the manufacturing and post-processing techniques. Before discussing manufacturing techniques of patterned surfaces, we will overview how the topography of functional surfaces should be appropriately characterized because it is crucial for understanding and giving insights into which length scales are relevant to specific functionalities. Furthermore, the realistic representation and characterization of surface roughness and topographic features are essential for modeling rough contact mechanics, mixed lubrication, adhesion, and convective heat transfer phenomena with greater accuracy.

Since the pioneering work in 1944[7] that first integrated surface decomposition (form, waviness, and roughness) and manufacturing signature, engineering surfaces have been conventionally treated as having a Gaussian (or at most, a bi-Gaussian) distribution of roughness heights, and parameters have been proposed to characterize the surface topography.[8] In most manufacturing contexts, a surface profile or areal topography is measured using stylus or optical profilometry. Then, mathematical operations are applied to the measured data to extract the level and the geometric form, remove outliers and separate the large-scale waviness and smallest-scale roughness using specific roughness filters.

In manufacturing, the surface topography is most commonly characterized using standardized parameters such as the arithmetical mean of the absolute roughness heights calculated from the reference mid-plane (or mid-line for surface profile), designated as S_a (or R_a for surface profile). The average roughness (R_a or S_a) for conventionally manufactured components ranges from 1 to 10 μm before polishing or finishing. However, recent additive manufacturing (AM) technologies produce roughness levels as high as 50 μm,[9] which can be advantageous to achieving certain functionalities, such as enhanced heat transfer.[10] Furthermore, the autocorrelation function (ACF) and the power spectrum density function (PSD) applied to surface topography can assess the self-affinity and the associated invariance of the surface roughness with the sampling interval.[11] However, these spectral methods do not deterministically represent the topography of a given surface as different surface configurations are possible for the same PSD.[12]

Traditional roughness filtering methods and parameters are inappropriate for surfaces with deep valleys, arrays of protruding features (pillars, fibrils, etc.), or discontinuous features. The standard Gaussian filter tends to cause significant distortions in the vicinity of features, but a robust Gaussian filter can mitigate the problem for plateau-type surfaces with a distribution of valleys (e.g., honed, laser-textured, or porous surfaces). With robust filters, the filter plane mostly follows the plateau, thus providing an unequivocal basis for the evaluation of plateau–valley structured surfaces.[13] Recently, the Spq parameter representing the plateau root-mean-square (RMS) height (instead of the global RMS, Sq) has been proposed for the characterization of honed surfaces due to their stratified structure,[13] but it can be extended to other functional surfaces. Other reformed indices have also been proposed to characterize the influences of texturing on functional properties.[14] Groove geometry and distribution and folded metal (material covering the grooves) should also be fully quantified because they directly affect the functionality of honed surfaces.

Components can have even higher apparent average roughness levels resulting from engineered surfaces containing deterministic patterns, such as dimples to improve tribological performance and ribs to promote turbulence and add surface area. In the other range, fairly smooth surfaces can be patterned, for example, with grooves (plateau honing)[13] to improve lubrication or with patterns of pillars or fibrils to increase adhesion and hydrophobicity.[2]

Topographic features in textured surfaces (e.g., dimples, pores, bumps, pillars, fibrils) require segmentation methods to separate the original topography into various surface components and scales that affect functional properties differently.[13] The promising concept of feature spectrum (see **Figure 1**) helps identify suitable surface-characterization methods for a wide range of surface topographies, establishing a unified methodology to correlate surface characterization, manufacturing, and surface functionality.[3] The left end of the spectrum is dominated by stochastic-based surfaces produced by conventional manufacturing processes, which can be characterized using conventional field parameters and statistical analysis. The right end of the spectrum is dominated by deterministic surfaces conceived to fulfil specific functionalities (surface texturing, fibril patterns, etc.), which

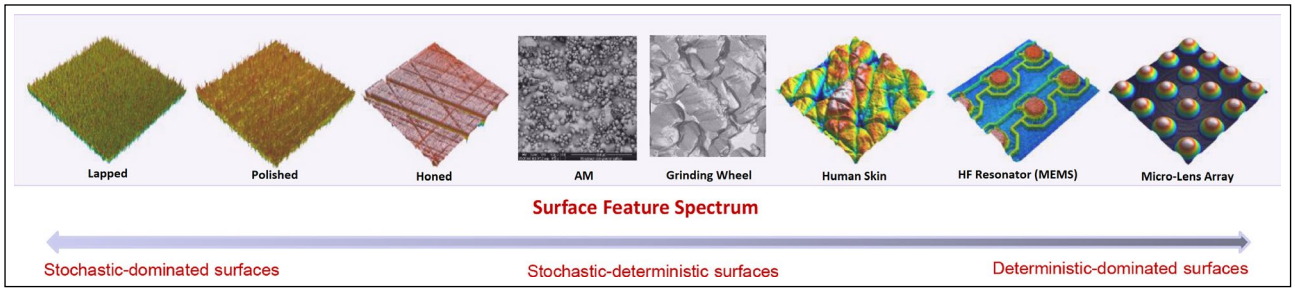

Figure 1. A spectrum of possible surface features. Reproduced with permission from Reference 3. AM, additive manufacturing; HF, high frequency; MEMS, microelectromechanical systems.

should be evaluated using more advanced featured-oriented characterization techniques based on segmentation methods that partition the original surface into different feature groups. The commonly used segmentation methods are the watershed segmentation with Wolf pruning, thresholding, edge detection, and statistical clustering. After the segmentation, the identified features (e.g., grooves, dimples, pockets, holes, channels, pillars, fibrils) are analyzed and characterized according to their attributes following specific standards or user-defined metrics. Feature-based characterization has been extended to the freeform topographies obtained with AM.[3]

Surface patterns on manufactured surfaces

This section discusses the surface patterns that can be obtained via different manufacturing technologies. First, it focuses on stochastic patterns resulting from conventional manufacturing. Next, we discuss technologies to produce specially designed deterministic surface textures with important applications in microfluidics, adhesion and friction control. Finally, we cover surfaces resulting from metal AM. Despite the usual trend of thinking of AM surfaces as problematic, we show that they are potentially useful and have been responsible for important recent advances in functional surfaces, particularly for improved convective heat transfer.

Surface patterns in conventional manufacturing

Conventional manufacturing of metallic components mostly involves cutting (turning, milling, drilling, etc.) or forming (drawing, rolling, stretching, bending), leading to relatively rough surfaces (1–10 μm), thus sometimes requiring the use of finishing techniques, mainly using abrasive methods (discussed in the following paragraph). Polymeric components are mostly manufactured by cast molding, thermoforming molding and extrusion, that lead to substantially smoother surfaces with a topography strongly correlated with the mold or forming tool topography.

The two most common abrasive finishing techniques are grinding and plateau honing. Grinding includes a group of finishing processes where the workpiece is tracked or rotated beneath an abrasive grinding wheel, forming channels oriented in the grinding direction, but this surface texture is not ideal for tribological applications. Plateau honing is widely used in internal-combustion engines to finish the surface topography of cylinder liners, creating a plateau-like surface with a cross-hatched pattern (third surface from the left in Figure 1) that strongly affects the friction/wear performance, fuel/oil consumption, and emissions of internal-combustion engines. Honed surfaces are composed of smooth load-bearing plateau areas and deep grooves that allow the storage of lubricant and wear particles, thus improving the lubrication control and retention.[13] Observation of surface topographies that are characteristic of manufactured components have suggested that further modification of surface topography could lead to optimized behavior. Improvements beyond the random texturing achieved through grinding and honing are discussed in the following section.

Surface texturing techniques

Surface texturing (or patterning or structuring) is a group of post-manufacturing technologies to produce deterministic patterns on a functional surface. It is challenging to manufacture the textures cheaply, fast, and reliably. This section describes the main surface techniques used today, with their advantages and shortcomings. A broader view of possible texturing techniques can be found in Reference 6.

Today, laser surface texturing (LST) is the most successful surface texturing technique for manufactured components. Etsion reviewed LST for tribological applications.[15] Since his pioneering work, the technique has evolved fast, with use in all the areas covered in this review (friction, adhesion, and convective heat transfer); a recent review shows the current trends and developments of LST.[16] It mostly involves localized material ablation via a focused, high-frequency pulsed laser beam. Alternatively, in direct laser interference patterning (DLIP), the textures result from self-reorganization of the surface as a response to localized heating. LST is very flexible in terms of materials, but involves substantial heating, possibly changing the local microstructures and mechanical properties, sometimes forming bulges that affect friction and wear.[5] Ultrashort pulsed lasers reduce the thermal impact to negligible values but at higher production costs.[16] Moreover, LST is

time-consuming (the texture is produced dimple-by-dimple), limiting large-scale production. This is reduced for DLIP, which directly patterns large areas with sub-micrometric textures at much higher speeds when the surfaces self-organize.[5]

The surface texture can also be formed by localized chemical or electrochemical material removal, often achieved via an insulating mask. Masking by photolithography results in accuracy and reproducibility, but at high cost and low texturing speed. Flexible photolithographic masks enable texturing of components with complex geometries at significantly lower costs.[17] For electrochemical removal (only applicable to conductive materials), ultrashort voltage pulses enhance the precision because dissolution is restricted to a region closer to the anode.[18] Alternatively, masking of the cathodic tool (instead of the anodic specimen) drastically reduces texturing time and costs because the masked cathode can be used to texture many workpieces, but the regions between the pockets are roughened.[19]

Patterns containing high-aspect-ratio motifs in relief, such as pillar and fibril patterns, could also be desired (see the section on adhesion and friction). Many fabrication techniques can fabricate pillars[6] or fibrillar patterned surfaces: replication, lithography, and micromachining.[2] The critical point of replication is to transfer the textures from a negative mold into the targeted soft materials. As for lithography or micromachining, it can produce textures by milling, drilling, etching of materials, or by additively curing photosensitive polymers. Different fabrication techniques can be chosen for different purposes. For scalable production and cost saving, many replication methods such as roll-to-roll processing, embossing, and microinjection molding can be adopted. For prototype validity and fundamental investigation, researchers prefer using techniques such as two-photon lithography, electron-beam lithography, and micromachining, after which the produced surfaces can further work as moldings for replication steps.

Surface patterns for additive manufacturing

Directed energy deposition processes for AM use a high-power energy source (electron beam or laser) to create a melt pool, to which either powder or wire feedstock are added. They can build components quickly, but at the cost of dimensional accuracy.[9] Laser sintering (LS) is one category of powder-bed fusion (PBF) to create small and highly detailed metallic features.[20] A thin layer of powder is spread over the build area, and each layer is subjected to a focused laser, leading to a much finer resolution than directed energy methods because it provides highly concentrated energy in a precise location.[21] For the laser, the user can control the speed, power, and scanning pattern. The interplay among all parameters requires complex parts to be printed in trials to determine the best combinations.[22] There are many nondimensional numbers and scaling parameters at play with laser-based AM.[23]

Figure 2 details the inherent roughness features of components using metal AM depending on processing parameters and component complexity, showing the range of surface morphologies for AM parts.[9] These surface morphologies result, for example, from partially melted particles to dross features, which consist of unwanted impurity material forming on the molten metal. As both the scanning speed and power increase, the melt pool elongates; as it becomes longer and narrower, Rayleigh instabilities occur, thus the melt pool breaks up into individual balls.[20] Reducing the laser power at any speed can result in a lack of fusion, which is increasingly important as the scanning speed increases. At the other extreme, excessively high laser power leads to surface defects. The key is to balance laser power and scanning speed within a region whereby conduction in the welding zone is maintained to control sintering. All of these types of roughness in Figure 2 can be tailored to enhance desired functionalities, such as heat-transfer characteristics,[9] as discussed later.

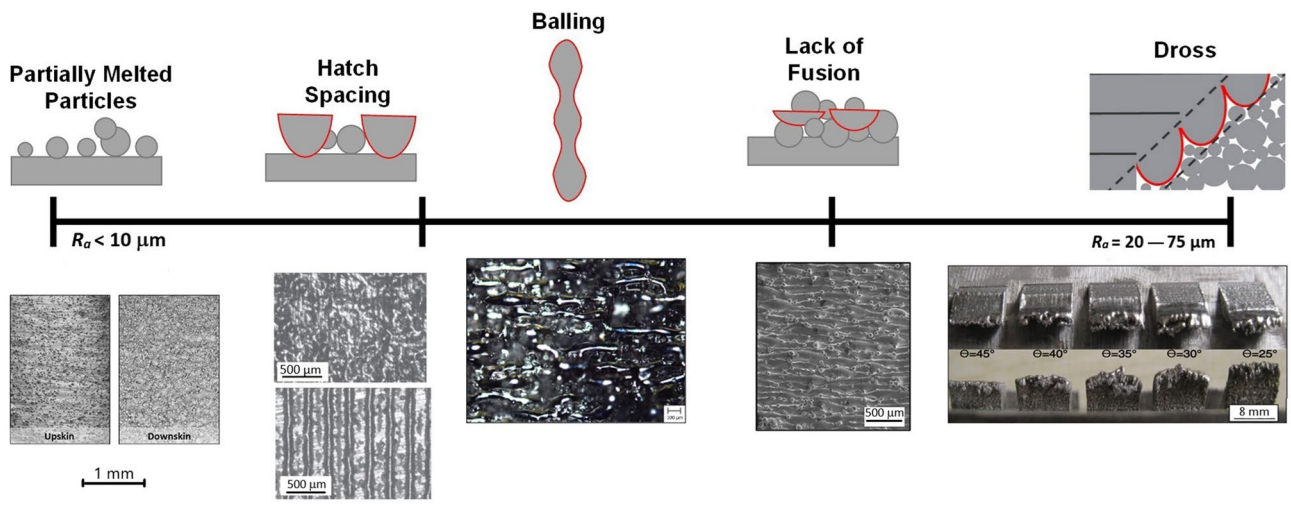

Figure 2. Morphology and roughness range impacted by additive manufacturing design and parameterization.

Dramatic differences in surface morphology can also result from the component build direction, defined as the angle from a surface to the plane of the powder bed.[24,25] With the complexity of the component geometries, inevitably not all surfaces can be printed in the same build direction. For microchannels built in different orientations, R_a values dramatically increase from 10 μm for a vertical build (perpendicular to powder layer) to 50 μm for a horizontal build (parallel to powder layer) due to gravitational effects on the sintered melt pool.[25]

Adhesion and friction of patterned surfaces

When surfaces come into contact, intermolecular (van der Waals interactions) between all solids inevitably lead to adhesion.[4] If a tangential force is present, adhesion is one of the components of friction according to the Bowden and Tabor model,[26] so often should be minimized to reduce costs, energy, and gas emissions. However, maximization of adhesion could be pursued, for example in the fabrication of adhesives or in the road/tire system.[16] Adhesion and friction are strongly dependent on surface topography, thus tunable by surface texturing. In tribological contacts, friction is dictated either by energy dissipation mechanisms at the asperity junctions or by lubricant shear. In addition to adhesion, the surface topography also controls other phenomena involved in friction, such as lubrication mechanisms. This section revises adhesion and friction of structured surfaces under dry and lubricated conditions.

Intermolecular adhesion in dry conditions

Between two atomically smooth surfaces, the adhesion force due to van der Waals forces is far stronger than what can be experienced in our daily life. For example, a contact area of 1 cm^2 (roughly the size of a 1-Euro coin) can theoretically hold a load of around 100 tons (much heavier than a small vehicle).[27] The real-world adhesion is quickly reduced because of the surface roughness or flaws, which increase the average separation distance of the components in contact and also drive earlier detachment through fracture processes.

Bioinspired fibril patterns are fascinating designs to suppress the attenuation of adhesion caused by the ubiquitous flaws. The fact that surfaces with fibrillar textures with less real contact area than a bulk surface can enhance adhesion is counterintuitive. Prior investigations into fibrillar patterns found in nature introduced the concept of contact splitting. Adhesion can be improved via contact splitting mainly due to crack trapping, increased surface-to-volume effect, adaptability to rough surfaces, and uniform stress distribution in the contact.[28] Patterns with pillars or fibrils can also increase hydrophobicity by adding an air–liquid interface that supports the droplets, reducing wetting. Hydrophobicity thus could additionally reduce adhesion, interfere with the formation of hydrodynamic lubricant films, as well as induce a so-called Marangoni effect (see later section on "Convective heat transfer").[2]

Thus, to enhance adhesion, many man-made surfaces have been engineered inspired by nature. Their adhesion can be modulated or enhanced by the presence of surface-patterned microstructures, (e.g., the gecko inspiration in dry adhesives and the octopus/tree frog inspiration in wet adhesives).[28] These synthetic bioinspired adhesive surfaces, although they leverage different dry- and wet-adhesion mechanisms, universally attach to targeted objects. In this section, we primarily review the progress in the micromechanical understanding of the origination of adhesion under dry and wet conditions. Then we expand from the single fibril design to the arrayed pattern, especially focusing on the statistical adhesion behavior of fibrillar arrays.

In 2000, Autumn et al.[29] terminated the debate on the origin of adhesion of submicron-sized gecko hairs. It was demonstrated to originate from van der Waals interactions instead of the suction effect. After that, intensive work came to emulate the gecko toe for engineering artificial patterned adhesive surfaces made of intrinsically nonsticky materials.[30]

The underlying mechanism is also investigated with an analogy to fracture mechanics. One representative model, a soft fibril with a diameter, D and Young's modulus, E adhering to a dissimilar stiff plane with a starter crack of length l, was recently proposed by Fleck et al.[31] for the prediction of the adhesion strength σ_p:

$$\sigma_p = \frac{0.6\sqrt{EW_{ad}}}{D^{0.406} l^{0.094} \widehat{a}}, \quad 1$$

where $\widehat{a}$ is a calibration factor of order 1 and W_{ad} the adhesion energy at the interface. A well-known contact-splitting effect occurs,[32] in which the adhesion stress progressively rises as the fibril size decreases. Eventually, the size effect diminishes in the flaw-insensitive regime where the dimension of the cohesive zone at the crack tip is comparable to the fibril size. The empirically determined predicted power-law index in Equation 1 (−0.406) has been verified experimentally.[33]

With the persistent pursuit of optimal adhesion via surface structuring (**Figure 3**), a mushroom-shaped modification on the tip of the fibril has largely outperformed cylindrical fibrils[34] (Figure 3a). With the mechanical explanation that the stress redistribution at the interface suppressed the edge-stress singularity, optimization routes have also been proposed. Another advanced strategy involves hierarchical structures (Figure 3b). Although their efficiency in terms of load sharing and resistance to defects has been theoretically demonstrated,[35] persuasive experiments are still missing due to manufacturing complexity.

Physical mechanisms controlling adhesion in wet conditions

In an aqueous environment, intermolecular interaction is attenuated due to the existence of a liquid film between the fibril and the counterface. Several physical mech-

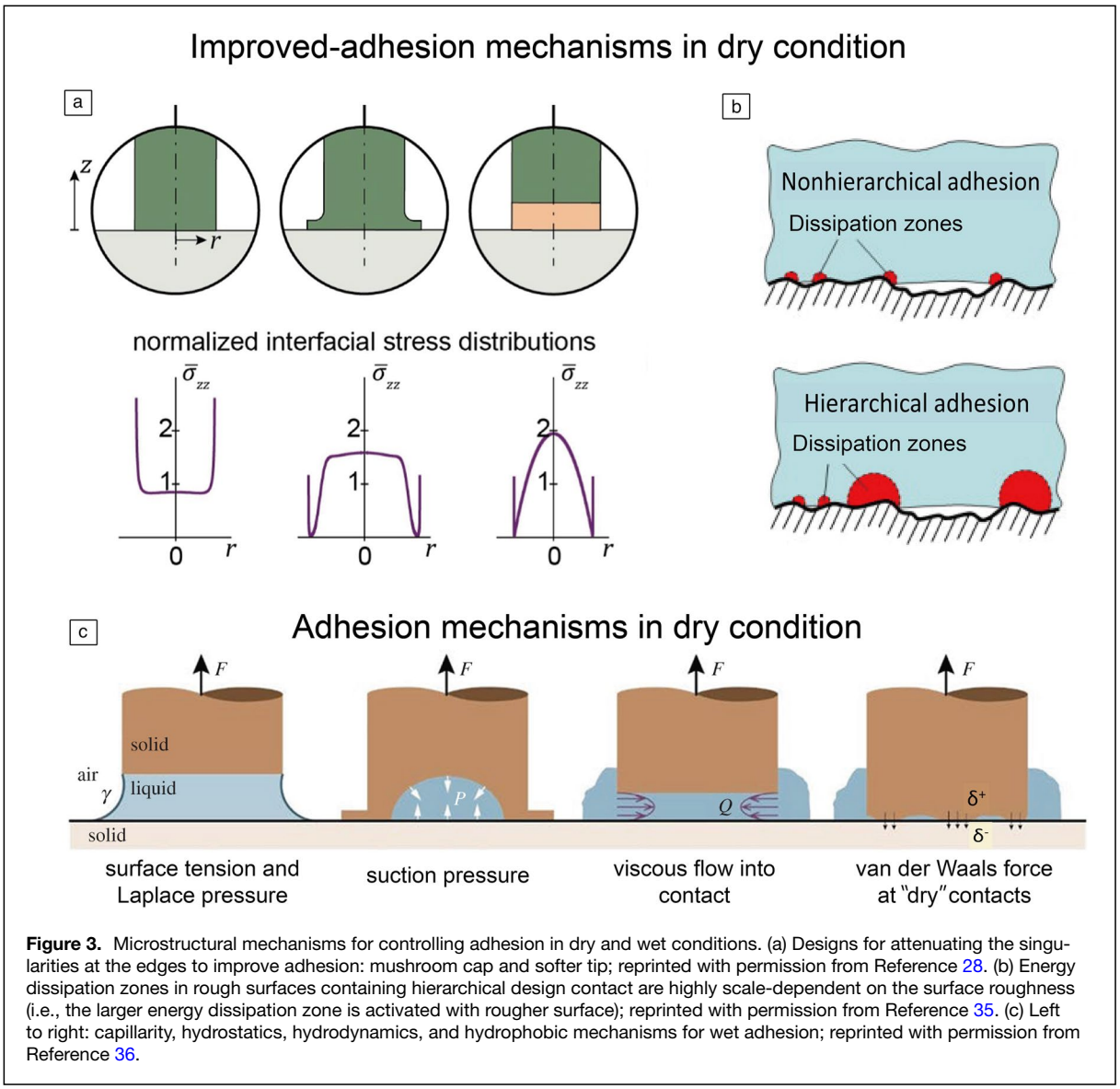

Figure 3. Microstructural mechanisms for controlling adhesion in dry and wet conditions. (a) Designs for attenuating the singularities at the edges to improve adhesion: mushroom cap and softer tip; reprinted with permission from Reference 28. (b) Energy dissipation zones in rough surfaces containing hierarchical design contact are highly scale-dependent on the surface roughness (i.e., the larger energy dissipation zone is activated with rougher surface); reprinted with permission from Reference 35. (c) Left to right: capillarity, hydrostatics, hydrodynamics, and hydrophobic mechanisms for wet adhesion; reprinted with permission from Reference 36.

anisms control adhesion in wet conditions (Figure 3c): capillarity, wet suction, and hydrodynamic force (or Stefan adhesion). The prerequisites for activating these forces are different. Capillarity needs a meniscus formed at three-phase junctions (solid–liquid–gas or liquid–liquid–solid). Thus, capillarity disappears when the structure wholly submerges into a homogeneous liquid. Stefan adhesion is only triggered by a viscous running liquid. Wet suction occurs if a pressure differential can be sustained inside and outside the suction, so it still functions for fully submerged fibrils and liquids with infinitesimal viscosity.[36]

Natural suction caps have attracted intense academic attention as one primary underwater adhesion strategy used by aquatic animals such as octopus and clingfish. A tilted cupped fibril bioinspired by the octopus showed wet adhesion >1 MPa (10× the atmosphere); this extremely high attachment has been recently attributed to the incompressibility of water. The theoretical stress is dominated by the cavitation pressure of water between 17 and 140 MPa, whereas the realistic stress is mediated by the buckling of the cup rim, leading to water leakage into the suction.[36] Alternatively, additional protuberances have been designed into the suction cup, also inspired by octopuses, increasing adhesion on moist and fully submerged substrates due to the assistance of capillary forces.[37] With their two-level microstructure at the toe pads, tree frogs show self-splitting and self-sucking effects, forming capillarity bridges that improve attachment.[38] Hydrodynamic adhesion physically originates from "dragging" the viscous liquid to fill the widening space during the separation of two objects. It was systematically studied by retracting a cylindrical fibril made of both soft and stiff materials from a substrate under different velocities.[39] Adding a mushroom cap onto a soft cylindrical fibril led to a transition from hydrodynamic to

hydrostatic adhesion along with a conceptual map of patterning design.

The fibril pattern usually contains hundreds or even thousands of single fibrils. The perfect adhesion of patterned fibrils is achieved only when each fibril detaches simultaneously with an evenly distributed adhesion strength (i.e., equal load sharing).[40] However, this is difficult to achieve due to practical factors such as misalignment or discrepancies among fibrils or contact conditions, so that large statistical variation in adhesion strength exists in a fibril array.

Recently, *in situ* experiments produced various insights into fibril adhesion: nearly one-third of fibrils already detach before reaching the adhesion strength; there is no obvious coupling effects between neighboring fibrils; and two crack modes—edge crack and center crack—facilitate detachment, where edge cracks are more common at earlier stages due to fabrication defects.[41] Weibull statistics and *in situ* observation of statistical data predict defect-dependent detachment strength and unstable detachment performance in compliant systems.[42]

Surface patterning for friction control

The modification of friction between moving surfaces is probably the most widely investigated application of surface texturing (more than 4500 articles can be found today in the database *Web of Science* since 2000 using the keywords "surface texturing" and "friction"). Despite this, a full understanding of the mechanisms involved under different tribological conditions and a clear definition of the effectiveness of surface textures are still lacking in the literature.[5] The main reasons for the lack of understanding and consensus are (1) the tribology of textured surfaces strongly depends on the contact conditions and lubrication regime; (2) the mechanisms operating in each condition differ, and sometimes authors incorrectly extrapolate conclusions obtained under conditions that are different from the intended application; (3) insufficient or inadequate use of simulation and analytical models, often leading to trial-and-error approaches; (4) surface texturing tends to change other surface characteristics (e.g., surface chemistry and microstructure), which indirectly affect tribological behavior, but are rarely characterized and discussed. This section provides the current state of the art in mechanisms for friction control using surface texturing.

The main challenge is that different mechanisms could operate depending on the contact and lubrication conditions, as summarized in **Figure 4**. The effects of surface texturing on dry friction have received much less attention than lubricated contacts. Different phenomena largely influenced by surface topography dissipate energy at the tribological interface during dry sliding, such as ploughing (by either the asperity contacts or wear debris), asperity adhesion, elastic/plastic deformation, and fracture. Thus, surface texturing can tune dry friction, as demonstrated by the early works by Suh et al.[43] Since then, investigations have attributed the lower dry friction of textured surfaces mainly to two mechanisms: (1) the entrapment of wear debris, which otherwise would plough the surfaces[44] (see debris stored inside the chevron-like pocket after dry sliding in Figure 4); and (2) the reduction of the real contact area, which reduce the adhesion component of friction (compare the contact of a conventionally machined surface against an ideally smooth counterbody with that for a textured surface in Figure 4c). Moreover, the textures alter the stress distribution in the contact region and its vicinities. The high contact pressures acting at the textures' edges (see the contact pressure distribution for a textured surface in Figure 4g) have hindered the use of surface texturing in dry contacts.[17] Because the surface textures tend to be quickly worn out under dry sliding, they are often combined with solid lubricant coatings.[45]

In the presence of a liquid lubricant, surface textures can act as micro-hydrodynamic bearings in mixed and (elasto) hydrodynamic lubrication conditions and increase the hydrodynamic film thickness. Because the film thickness is inversely proportional to the applied load, textured contacts could support higher loads with thicker average film thickness without asperity contact (i.e., higher load-bearing capacity [Figure 4h]).[46,47] This micro-hydrodynamic bearing effect is induced by the lubricant cavitation in the divergent portion of the textures. Furthermore, this localized cavitation can also contribute to sucking more lubricant into the contact[48] due to the pressure difference between the cavitated zone and the lubricant in the vicinity, a phenomenon known as inlet suction (Figure 4f).[49] Textures can also function as micro-reservoirs of lubricant and, in combination with the inlet suction effect, supply additional lubricant into the contact, thus mitigating lubricant starvation,[48,49] as shown for metal forming in Figure 4. Recently, strong experimental evidence showed a new mechanism under full-film lubrication (e.g., at mid-stroke for the piston–liner system) named as shear area variation (Figure 4), in which the area where lubricant shear occurs changes over the textures, and the lubricant shear stress is reduced.[50] Under boundary lubrication, surface texturing can favor the tribochemical reactions involved in forming protective boundary tribofilms from additives present in the lubricant,[5,51] leading to enhanced tribofilm formation (Figure 4g).

Despite the potential benefits of surface texturing to reduce friction, it is very rarely used in rolling machine elements. Rolling surfaces are prone to rolling contact fatigue (RCF), a wear mode caused by the coalescence and growth of microscopic fatigue cracks initiated by local cyclic plastic deformation around the surface asperities. Thus, smooth surfaces normally perform better in rolling contacts and surface texturing is rarely used. However, the valleys in a textured surface could decrease the interaction between asperities, positively affecting RCF life. Improved lubrication can also potentially increase RCF life for textured surfaces, as shown for the wheel–rail system in Figure 4.[52]

Certain applications could also require friction to be maximized, such as brakes, clutches, transmission systems, and the road–tire contact, also tunable by the control of the surface topography. For compliant surfaces, texturing can increase the real contact area and the adhesion component of friction

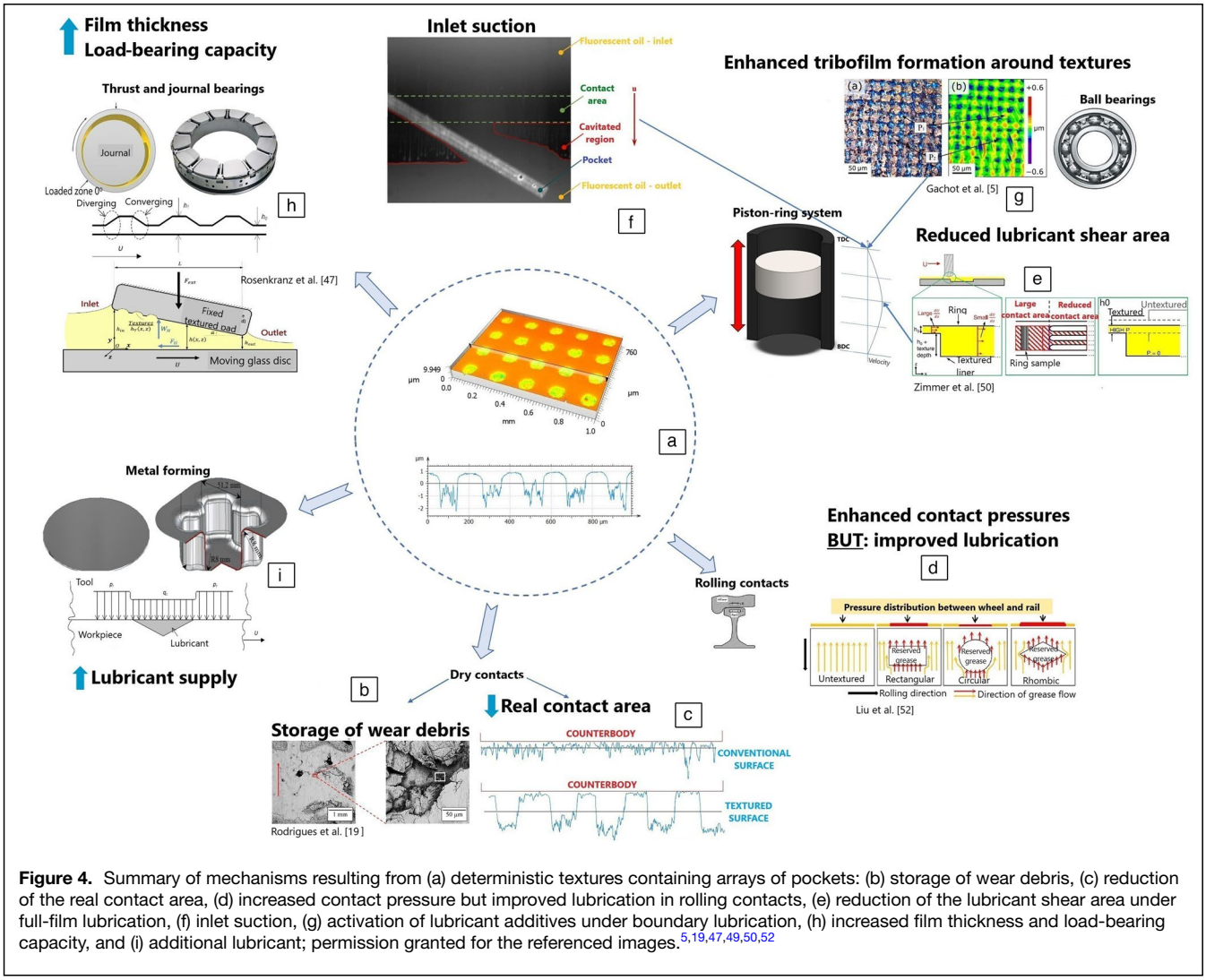

Figure 4. Summary of mechanisms resulting from (a) deterministic textures containing arrays of pockets: (b) storage of wear debris, (c) reduction of the real contact area, (d) increased contact pressure but improved lubrication in rolling contacts, (e) reduction of the lubricant shear area under full-film lubrication, (f) inlet suction, (g) activation of lubricant additives under boundary lubrication, (h) increased film thickness and load-bearing capacity, and (i) additional lubricant; permission granted for the referenced images.[5,19,47,49,50,52]

(due to contact splitting), thus increasing friction. If a liquid is present, directional textures can suppress hydrodynamic lubrication by channeling the liquid away from the contact (e.g., reducing skid in the road–tire contact). Other important mechanisms to increase friction via the surface topography are mechanical interlocking and the increase of the deformation component of friction. Directional textures (e.g., parallel channels or protruding stripes) can potentially increase direction in one direction and reduce friction in the perpendicular direction (anisotropic friction).[16]

Effects of surface topography on convective heat transfer

In heat-transfer contexts, structured surfaces increase the contact area between the coolant and the solid surface, increasing convective heat transfer. Textured surfaces have enabled the development of heat exchangers that function by spray cooling, where a phase change (vapor) is produced at the surface, making heat removal much easier than for a liquid. Boiling heat transfer is another possibility, where structured surfaces create nucleation sites for the creation of vapor bubbles at the heating surface. In microfluidics, structured surfaces could induce thermocapillary effects. Because patterns of high-aspect-ratio features can increase hydrophobicity, a combination of textured and untextured regions can induce mass transfer along the interface between the solid and liquid due to the surface-tension gradient (Marangoni effect), increasing convective heat transfer.[2] For a detailed analysis of micro- and nanometric textures on microfluidics and thermocapillary, the reader is directed to other reviews.[2,53]

At the other end of the size range, large surface structures produced by AM have large potential to control fluid frictional losses and convective heat transfer. Given the advances in 3D metal printing that provide a platform for innovation, the pressure loss and heat-transfer augmentations relative to that occurring in a smooth channel are significantly higher. In fact, the range of augmentations of an additively manufactured surface overlaps with that of a highly engineered surface, highlighting the importance of the roughness and the opportunities for exploiting additively manufactured components.

Modeling and simulation of the effects of surface patterns on properties

The design process of high-performance functional surfaces can be significantly improved with numerical simulation analysis, allowing the prediction of the interplay between a variety of multiscale and multiphysics phenomena (e.g., fluid flow and cavitation, complex rheology, heat transfer and thermal effects, asperity contact, surface wettability, adhesion, percolation) taking place simultaneously on different length and time scales.[54] Furthermore, numerical results can help shed light on the underlying mechanisms responsible for governing the friction, wear, adhesion, failure modes, and convective heat transfer in a variety of applications, thus contributing to the tailoring of novel surface engineering technologies.

Dry and wet adhesion

Multiple mechanisms control the adhesion in dry or wet conditions, and two approaches—continuum mechanics-based finite element methods (FEMs) and molecular dynamics simulations—are frequently used for modeling and providing quantitative analyses on adhesion behaviors at different length scales.

Recent modeling studies using FEM simulations have demonstrated that the critical point for enhancing the adhesion is to optimize the interfacial stress distribution by reducing the corner stress singularity. These investigations have numerically shown a significant reduction in edge stresses, suggesting new designs with improved adhesion, such as fibrils with a mushroom cap or softer tip, compared to a cylinder fibril.[55] Additionally, by introducing the cohesive zone model into the simulations, tensile stress can be captured in the numerical analyses, and an optimal mushroom-cap thickness on adhesion was proposed and verified with experimental demonstration.[55] Promisingly, many groups worldwide have developed a variety of methods for small-scale simulations able to solve complex contact problems,[56] which optimistically provide us with powerful tools to simulate contact problems with patterned surfaces, either to maximize adhesion for the optimization of adhesive surfaces or to understand and minimize the adhesion component of friction in dry contacts.

Fibril patterning statistics were earlier analyzed by the Monte Carlo technique assuming normal/uniform probabilities for the distribution of fibril lengths.[57] As an analogy to the rupture of brittle solids, a mechanical model showed that the fibril detachment was dominated by the weakest link defects.[58]

Mixed lubricated contacts

Many lubricated (bio)mechanical components subjected to severe contact conditions (e.g., rolling bearings, gears, piston rings, human joints) fully or partially operate in the mixed lubrication regime, where the lubricant film thickness cannot fully separate the asperities of the contacting surfaces. Thus, lubricant films and direct rough-surface–asperity contacts coexist, sharing the applied load, so the effects of the surface topography on both contact asperity and lubrication need to be considered to optimize the tribological performance.

Although the effects of surface topography on full-film lubrication have been well reviewed in the literature,[59] extensive reviews devoted to modeling and simulation of mixed lubrication are scarce, and this section is intended to cover this gap partially. In the last decades, substantial advances in mathematical and numerical models for predicting the mixed lubrication behavior between rough surfaces fabricated by different manufacturing processes have been achieved. Essentially, two modeling approaches have been used depending on how the topography is considered in the governing equations: the averaging/homogenization-based methods and deterministic modeling.

In averaging and homogenization methods, the global effect of topography on lubrication is considered using specific coefficients in the governing lubrication equations defined over the entire contact interface. These coefficients (flow factors or homogenization coefficients) scale up the microscopic effects on lubricant flow into component-scale models solved considering the macroscopic geometry of the contact using either averaged or homogenized Reynolds equation forms.

Early studies mainly applied the stochastic process theory yielding a stochastic Reynolds equation for the mean (or expected) fluid pressure.[60] Later, Patir and Cheng[61] proposed a pioneering average flow model that locally averaged the lubricant flow at the microscopic roughness scale, resulting in an averaged Reynolds equation expressed in terms of flow factors, thus capturing the influence of roughness on the macroscopic domain. The flow factors are calculated *a priori* by deterministically solving the mixed lubrication problem at the microscopic scale on a statistical ensemble of rough bearing cells. Patir and Cheng's model provides accurate average pressure distributions for isotropic and orthotropic surface topographies. The limitation of the model on dealing with cross-flow in anisotropic surfaces is mitigated using an extended generalized tensorial form of the average flow model.[62] Since then, other averaging methods have been proposed, such as the volume averaging method that combined spatial and time averaging and accounted for the unlubricated contact areas.[63] The homogenization theory is another approach for modeling fluid flow between rough surfaces in a more rigorous mathematical framework. Homogenization methods overcome the inherent empirical aspect of the local flow correction at the microscopic scale in Patir and Cheng's average flow model by defining more appropriate boundary conditions for solving the microscale problem.[64]

Comparing the homogenization model and the Patir and Cheng's model, the incorrect boundary conditions at the microscale for Patir and Cheng's model result in significant deviations of the averaged pressure distributions, but only for nonsymmetric surface patterns. Another ill-explored advantage of homogenization methods is that it allows the upscaling of the average pressure solutions to retrieve microscale information,

enabling more accurate predictions of performance parameters (e.g., peak pressure and friction).[65] Moreover, the homogenization approach is not restricted to periodic roughness and can be extended by reiterated homogenization,[66] providing a computationally efficient strategy to evaluate surfaces that are rough and textured. Therefore, considering the negligible additional computation effort and implementation complexity, homogenization should be the preferred method to deal with surface topographies with arbitrary patterns. An overview of modeling and numerical methods to handle rough and textured surfaces can be found in Reference 67. Finally, because in the mixed lubrication regime the load is sustained by both the lubricant and the asperities, when either averaging or homogenization methods are used, stochastic rough contact models or stiffness contact curves obtained from deterministic calculations are often employed to evaluate the corresponding average asperity contact pressure distributions.[68]

Because the averaging and homogenization methods deal with the global effects of surface topography, they are usually unable to provide detailed information about local deviations of quantities that are critical to understanding lubrication breakdown and failure mechanisms (e.g., severe contact pressures and stress fields, minimum film thickness, flash temperature, etc.). In recent decades, advances in computing power and more efficient numerical techniques have enabled the development of deterministic methods for modeling mixed lubrication problems. This approach allows the direct use of real engineering surfaces in numerical simulations through a full-scale representation of the surface topography in the lubricant film geometry. The hydrodynamic and asperity contact problems are simultaneously solved in the same solution framework, thus providing localized lubrication and microcontact details. However, the computational effort is high due to the higher mesh resolution required to represent the microscale geometry.

A pioneering deterministic transient mixed lubrication model proposed a partitioned solution with hydrodynamic and asperity contact pressures calculated separately, then updated in sequential iterations. A multigrid method solved the Reynolds equation for the fluid pressure in the lubricated regions and an FFT procedure calculated the asperity contact pressures.[69] Later, a fully coupled unified framework improved solution convergence and stability, treating the lubricated and asperity contact regions simultaneously in a unified system of equations, where the hydrodynamic and contact pressures are updated within the same iteration step.[70] Further improvements to the model included thermal effects, plastoelasticity, interasperity cavitation, and starvation.[71]

Deterministic mixed lubrication simulations have also been used to explain the experimentally observed hydrodynamic pressure generation between parallel rough surfaces. Recently, it was attributed to the transverse pumping mechanism, arising from the collective effect of local lateral lubricant flow induced by roughness, which should be balanced by additional pressure flow to ensure mass conservation. Subsequently, a deterministic model[72] based on Hu and Zhu's unified approach[70] included the interaction between asperities and the influence of the fluid pressure on asperity deformation (micro-EHL effect), and showed that this was a critical mechanism affecting the fluid pressure buildup between parallel rough surfaces. Inspired by a scaling methodology that provides an efficient computational strategy to use deterministic simulation results in full-cycle engine simulations of the piston ring—cylinder liner system, a deterministic model, including interasperity cavitation was applied to oil control rings of an internal-combustion engine. The model predicted significant hydrodynamic load capacity due to the interplay between the fluid pressure buildup around asperities and honing grooves.[73] It is important to remark that because the averaging or homogenization models need separate deterministic models to determine flow factors or homogenization coefficients for specific surface topographies, deterministic mixed lubrication models play a crucial role in accurate lubrication analysis.

Convective heat transfer

The correlations that have been presented in the literature traditionally have built upon the concept of using Colebrook's original formulation of a sand grain roughness (k_s) in which the physical surface characterization of the roughness (R_a) is correlated to that of a sand grain roughness. The correlation between R_a and k_s is developed through a direct measure of channel pressure losses. Once this relationship is known, the correlations first presented by Stimpson et al.[74] can be used to predict the resulting heat transfer:

$$\frac{1}{\sqrt{f}} = -2.0\log\left(\frac{k_s/D_h}{3.7} + \frac{2.51}{\mathrm{Re}\sqrt{f}}\right), \tag{2}$$

$$\mathrm{Nu} = \frac{\left(\mathrm{Re}^{0.5} - 29\right)\mathrm{Pr}\sqrt{\frac{f}{8}}}{0.6\left(1 - \mathrm{Pr}^{2/3}\right)}. \tag{3}$$

Although only limited data sets were used in Reference 74 to develop these correlations, a significant number of subsequent studies were completed and included to improve upon the correlation that relates k_s to R_a,[9] given by:

$$\frac{K_s}{D_h} = 11\frac{R_a}{D_h}. \tag{4}$$

The modeling and simulation of the effects of surface topography on convective heat transfer for conventionally manufactured surfaces traditionally consider that the surface roughness is very small when compared with the thickness of the boundary layer.[75] However, the recent trend of using the surfaces produced by AM to enhance convective heat transfer in heat exchangers deals with much rougher surfaces. Asperity heights are on the order of 500 μm or even more, with a size scale comparable to the cooling channel features or even the channel height. Given the complexity and randomness of the roughness characteristics brought about by AM,

computational models simulating such phenomena are challenging. Two-equation turbulence models, used for many simulations, assume a laminar sublayer with logarithmic behavior of the near-wall velocity profile; however, with roughness levels representative of AM, such behavior is questionable. The simulations shown by Altland et al.[75] were the first to use direct numerical simulations (no wall modeling) of relevant roughness levels, which indicated that the logarithmic behavior does exist. They used their data to validate further the use of a roughness sheltering model presented by Yang et al.[76] and showed better success predicting the velocity profiles than the typical algebraic model. Although these modeling efforts showed success, more research is needed to evaluate the models needed for the energy equation to predict heat transfer from an additively manufactured surface accurately.

Knowledge gaps, future trends, and design guidelines

The understanding of fundamental mechanisms has been elaborated massively for controlling or improving surface functionalities by micropatterning strategies, but we still stay far from completeness.

Patterned adhesive surfaces evolved by understanding the adhesion of patterned surfaces in nature. However, a real gecko displays a versatile adhering and clinging ability not yet fully realized by artificial fabrication techniques. A typical characteristic in animal feet—the hierarchical microstructures with feature sizes down to hundreds of nanometers—still lacks experimental investigation due to manufacturing complexity. Additionally, the field still lacks the realization of optimized reliable micropatterning designs for adhering to arbitrarily curved rough surfaces. Another challenge is the growing demand for automated manipulation of micro-objects in industrial miniaturization. Opposite to pursuing high adhesion, specialized surfaces are required that combine adhesion and releasing ability on demand. So far, robots equipped with patterned adhesives have been designed for locomotion or manipulator tasks, such as the StickyBot and FarmHand by the Cutkosky Lab, achieving a climbing speed of centimeters/second or pick-and-place-grasping of complex-shaped objects.[77] Also, due to the high conformability of the fibril-patterned adhesives to curved or rough surfaces, wearable sensors for monitoring pressure, temperature, ECG signal, and motion detection are emerging.

Despite the current understanding of how surface topography and topographic features affect friction under dry and lubricated contacts, mostly by boosting different additional lubrication mechanisms and entrapping wear debris, certain areas still require further advancements in understanding. Two such areas are the determination of how surface patterns control wear, and the tribochemical processes governing the activation of boundary films formed from lubricant additives. Furthermore, understanding percolation effects, triboelectric contacts, and the interplay between thermal effects, complex lubricant rheology and material inhomogeneity in mixed lubrication all require attention in future research. All of these challenges require the application of multiphysics and multiscale modeling and simulation approaches, as well as advanced experimentation, to accurately capture such microscale-controlled effects on the macroscale performance of engineering components. Particularly, developing asperity-based mixed lubrication models that account for elastoplasticity, asperity interaction, and substrate deformation is a promising strategy to achieve computationally efficient simulations for applications requiring rapid design.

For convective heat transfer, frontier challenges include the combined analysis of all the complex mechanisms involved in convective heat transfer, such as fluid mechanics and pressure loss, surface tension, phase-change nucleation, and heat transfer. For the new AM surfaces, the large structures pose further difficulties to the fluid mechanics, so only very recently, attempts to model convective heat transfer as a function of surface topography have started and should receive a strong focus in further studies.

Finally, the rapid development in computer technology and data science should facilitate the methodology for designing novel micropatterns using data-driven and physics-informed machine learning approaches to improve all the surface functionalities addressed in this article.

Data availability

Not applicable.

Conflict of interest

On behalf of all authors, the corresponding author states that there is no conflict of interest.

References

1. A. Gujrati, S.R. Khanal, L. Pastewka, T.D.B. Jacobs, *ACS Appl. Mater. Interfaces* **10**(34), 29169 (2018)
2. A.A.G. Bruzzone, H.L. Costa, P.M. Lonardo, D.A. Lucca, *CIRP Ann.–Manuf. Technol.* **57**(2), 750 (2008)
3. X. Jiang, N. Senin, P.J. Scott, F. Blateyron, *CIRP Ann.–Manuf. Technol.* **70**(2), 681 (2021)
4. B.N.J. Persson, *Phys. Rev. Lett.* **87**, 116101 (2001)
5. C. Gachot, A. Rosenkranz, S.M. Hsu, H.L. Costa, *Wear* **372–373**, 21 (2017)
6. H.L. Costa, I.M. Hutchings, *Proc. Inst. Mech. Eng. J J. Eng. Tribol.* **229**(4), 429 (2015)
7. R.E. Reason, M.R. Hopkins, R.I. Garrod, *Report on the Measurement of Surface Finish by Stylus Methods* (Taylor, Taylor & Hobson, Leicester, 1944)
8. L.D. Todhunter, R.K. Leach, S.D.A. Lawes, F. Blateyron, *CIRP J. Manuf. Sci. Technol.* **19**, 84 (2017)
9. K.A. Thole, S.P. Lynch, A.J. Wildgoose, "Review of Advances in Convective Heat Transfer Developed through Additive Manufacuring," in *Advances in Heat Transfer* (Elsevier, Amsterdam, 2021), vol. 53, chap. 5, pp. 249–325
10. J.C. Snyder, K.A. Thole, *J. Turbomach.* **142**, 051007 (2020)
11. D.J. Whitehouse, J.F. Archard, *Proc. R. Soc. Lond. A* **316**(1524), 97 (1970)
12. T.D.B. Jacobs, T. Junge, L. Pastewka, *Surf. Topogr.* **5**(1), 013001 (2017)
13. P. Pawlus, R. Reizer, *Tribol. Int.* **167**, 107409 (2022)
14. H. Yue, J. Deng, J. Schneider, *Surf. Topogr.* **9**(3), 035013 (2021)
15. I. Etsion, *J. Tribol. Trans. ASME* **127**, 248 (2005)
16. H.L. Costa, J. Schille, A. Rosenkranz, *Friction* **10**(9), 1285 (2022)
17. S.M. Hsu, Y. Jing, F. Zhao, *Surf. Topogr.* **4**(1), 014004 (2016)
18. X. Chen, N. Qu, H. Li, Z. Xu, *Appl. Surf. Sci.* **343**, 141 (2015)
19. T.A. Rodrigues, R.V. Arencibia, H.L. Costa, W.M. da Silva, *Surf. Topogr.* **8**(2), 024011 (2020)
20. J.-P. Kruth, G. Levy, F. Klocke, T.H.C. Childs, *CIRP Ann.–Manuf. Technol.* **56**(2), 730 (2007)
21. D. Wang, Y. Yang, Z. Yi, X. Su, *Int. J. Adv. Manuf. Technol.* **65**, 1471 (2013)
22. I. Yadroitsev, I. Smurov, *Phys. Procedia* **12**, 264 (2011)

23. T. Mukherjee, V. Manvatkar, A. De, T. DebRoy, *J. Appl. Phys.* **121**, 064904 (2017)
24. J.C. Snyder, C.K. Stimpson, K.A. Thole, D.J. Mongillo, *J. Mech. Des.* **137**(11), 111411 (2015)
25. A.J. Wildgoose, K.A. Thole, P. Sanders, L. Wang, "Impact of Additive Manufacturing on Internal Cooling Channels with Varying Diameters and Build Directions," in *Turbo Expo: Power for Land, Sea, and Air, 2020, Vol. 7A: Heat Transfer* (American Society of Mechanical Engineers, 2020), paper no. V07AT15A017
26. F.P. Bowden, D. Tabor, *The Friction and Lubrication of Solids* (Oxford University Press, Oxford, 2001)
27. V.L. Popov, *Contact Mechanics and Friction* (Springer, Berlin, 2010)
28. E. Arzt, H. Quan, R.M. McMeeking, R. Hensel, *Prog. Mater. Sci.* **120**, 100823 (2021)
29. K. Autumn, Y.A. Liang, S.T. Hsieh, W. Zesch, W.P. Chan, T.W. Kenny, R. Fearing, R.J. Full, *Nature* **405**, 681 (2000)
30. R. Hensel, K. Moh, E. Arzt, *Adv. Funct. Mater.* **28**(28), 1800865 (2018)
31. N.A. Fleck, S.N. Khaderi, R.M. McMeeking, E. Arzt, *J. Mech. Phys. Solids* **101**, 30 (2017)
32. E. Arzt, S. Gorb, R. Spolenak, *Proc. Natl. Acad. Sci. U.S.A.* **100**(19), 10603 (2003)
33. C. Greiner, A. del Campo, E. Arzt, *Langmuir* **23**(7), 3495 (2007)
34. L. Heepe, S.N. Gorb, *Annu. Rev. Mater. Res.* **44**, 173 (2014)
35. H. Yao, H. Gao, *Int. J. Solids Struct.* **44**, 8177 (2007)
36. Y. Wang, Z. Li, M. Elhebeary, R. Hensel, E. Arzt, M.T.A. Saif, *Sci. Adv.* **8**, eabm9341 (2022)
37. S. Baik, D.W. Kim, Y. Park, T.-J. Lee, S.H. Bhang, C. Pang, *Nature* **546**, 396 (2017)
38. F. Meng, Q. Liu, X. Wang, D. Tan, L. Xue, W.J.P. Barnes, *Philos. Trans. A Math. Phys. Eng. Sci.* **377**(2150), 20190131 (2019)
39. Y. Wang, R. Hensel, E. Arzt, *J. R. Soc. Interface* **19**(189), 20220050 (2022)
40. C.Y. Hui, N.J. Glassmaker, T. Tang, A. Jagota, *J. R. Soc. Interface* **1**(1), 35 (2004)
41. V. Tinnemann, L. Hernández, S.C.L. Fischer, E. Arzt, R. Bennewitz, R. Hensel, *Adv. Funct. Mater.* **29**(14), 1807713 (2019)
42. R. Hensel, J. Thiemecke, J.A. Booth, *ACS Appl. Mater. Interfaces* **13**(16), 19422 (2021)
43. N.P. Suh, M. Mosleh, P.S. Howard, *Wear* **175**(1–2), 151 (1994)
44. A. Rosenkranz, L. Reinert, C. Gachot, F. Mücklich, *Wear* **318**(1–2), 49 (2014)
45. A. Rosenkranz, H.L. Costa, M.Z. Baykara, A. Martini, *Tribol. Int.* **155**, 106792 (2021)
46. H.L. Costa, I.M. Hutchings, *Tribol. Int.* **40**(8), 1227 (2007)
47. A. Rosenkranz, H.L. Costa, F. Profito, C. Gachot, S. Medina, D. Dini, *Tribol. Int.* **134**, 190 (2019)
48. H.L. Costa, I.M. Hutchings, *J. Mater. Process. Technol.* **209**, 1175 (2009)
49. S.-C. Vladescu, A.V. Olver, I.G. Pegg, T. Reddyhoff, *Tribol. Int.* **82** (Pt. A), 28 (2015)
50. M. Zimmer, S.-C. Vlădescu, L. Mattsson, M. Fowell, T. Reddyhoff, *Tribol. Int.* **161,** 107067 (2021)
51. L.C. Dias, G. Pintaude, A.A.O.F. Vittorino, H.L. Costa, *Lubricants* (Basel) **10**(6), 118 (2022)
52. J.-H. Liu, P.-J. Yu, Y.-J. Zhou, Z.-B. Xu, Y.-J. Li, P. Li, Z. Zhao, C.-G. He, M.-X. Shen, *Wear* **498–499**, 204310 (2022)
53. P.G. Grützmacher, S.V. Jalikop, C. Gachot, A. Rosenkranz, *Surf. Topogr.* **9**, 013001 (2021)
54. A.I. Vakis, V.A. Yastrebov, J. Scheibert, L. Nicola, D. Dini, C. Minfray, A. Almqvist, M. Paggi, S. Lee, G. Limbert, J.F. Molinari, G. Anciaux, R. Aghababaei, S.E. Restrepo, A. Papangelo, A. Cammarata, P. Nicolini, C. Putignano, G. Carbone, S. Stupkiewicz, J. Lengiewicz, G. Costagliola, F. Bosia, R. Guarino, N.M. Pugno, M.H. Müser, M. Ciavarella, *Tribol. Int.* **125**, 169 (2018)
55. X. Zhang, Y. Wang, R. Hensel, E. Arzt, *J. Appl. Mech.* **88**, 031015 (2020)
56. M.H. Müser, W.B. Dapp, R. Bugnicourt, P. Sainsot, N. Lesaffre, T.A. Lubrecht, B.N.J. Persson, K. Harris, A. Bennett, K. Schulze, S. Rohde, P. Ifju, W.G. Sawyer, T. Angelini, H.A. Esfahani, M. Kadkhodaei, S. Akbarzadeh, J.-J. Wu, G. Vorlaufer, A. Vernes, S. Solhjoo, A.I. Vakis, R.L. Jackson, Y. Xu, J. Streator, A. Rostami, D. Dini, S. Medina, G. Carbone, F. Bottiglione, L. Afferrante, J. Monti, L. Pastewka, M.O. Robbins, J.A. Greenwood, *Tribol. Lett.* **65**, 118 (2017)
57. P.K. Porwal, C.Y. Hui, *J. R. Soc. Interface* **5**, 441 (2008)
58. R.M. McMeeking, E. Arzt, A.G. Evans, *J. Adhes.* **84**(7), 675 (2008)
59. D. Gropper, L. Wang, T.J. Harvey, *Tribol. Int.* **94**, 509 (2016)
60. L.S.H. Chow, H.S. Cheng, *J. Lubr. Technol.* **98**, 117 (1976)
61. N. Patir, H.S. Cheng, *J. Lubr. Technol.* **101**, 220 (1979)
62. J.H. Tripp, *J. Lubr. Technol.* **105**, 458 (1983)
63. M. Prat, F. Plouraboué, N. Letalleur, *Transp. Porous Media* **48**, 291 (2002)
64. A. Almqvist, J. Fabricius, P. Wall, *J. Math. Anal. Appl.* **390**(2), 456 (2012)
65. M. Rom, F. König, S. Müller, G. Jacobs, *Appl. Eng. Sci.* **7**, 100055 (2021)
66. A. Almqvist, E.K. Essel, J. Fabricius, P. Wall, *Proc. Inst. Mech. Eng. J J. Eng. Tribol.* **222**(7), 827 (2008)
67. P.G. Grützmacher, F.J. Profito, A. Rosenkranz, *Lubricants* (Basel) **7**(11), 95 (2019)
68. R.I. Taylor, *Lubricants* (Basel) **10**, 98 (2022)
69. X. Jiang, D.Y. Hua, H.S. Cheng, X. Ai, S.C. Lee, *J. Tribol.* **121**(3), 481 (1999)
70. D. Zhu, Y.-Z. Hu, *Tribol. Trans.* **44**(3), 383 (2001)
71. Q.J. Wang, D. Zhu, *Interfacial Mechanics: Theories and Methods for Contact and Lubrication* (CRC Press, Boca Raton, 2019)
72. Y. Wang, A. Azam, G. Zhang, A. Dorgham, Y. Liu, M.C.T. Wilson, A. Neville, *Lubricants* (Basel) **10**(1), 12 (2022)
73. F.J. Profito, E. Tomanik, D.C. Zachariadis, *Tribol. Int.* **93** (Pt. B), 723 (2016)
74. C.K. Stimpson, J.C. Snyder, K.A. Thole, D. Mongillo, *J. Turbomach.* **138**(5), 051008 (2016)
75. S. Altland, X. Zhu, S. McClain, R. Kunz, X. Yang, *Flow* (Camb.) **2**, E19 (2022)
76. X.I.A. Yang, J. Sadique, R. Mittal, C. Meneveau, *J. Fluid Mech.* **789**, 127 (2016)
77. W. Ruotolo, D. Brouwer, M.R. Cutkosky, *Sci. Robot.* **6**(61), eabi9773 (2021) □

Henara L. Costa is a full professor at the Federal University of Rio Grande, Brazil, where she is the Head of the Surface Engineering Group. She is also the coordinator of the National Institute on Green Tribology for the Energy Transition. She obtained her PhD degree from the University of Cambridge, UK. She has worked with tribology for more than 25 years, with a main focus on reducing friction losses using surface modification and coatings or lubrication. Costa has authored approximately 200 manuscripts in journals, book chapters, and conference proceedings. She is the editor-in-chief for *Surface Topography: Metrology and Properties*, a member of the International Federation for the Promotion of Mechanism and Machine Science (IFToMM), and the Brazilian Representative at the International Energy Agency-Advanced Materials for Transportation (IEA/AMT). Costa can be reached by email at henaracosta@furg.br.

Francisco J. Profito is an assistant professor in mechanical engineering at the Polytechnic School of the University of São Paulo, Brazil. He was a visiting doctoral researcher at Imperial College London, UK, from 2014 to 2015. He has developed modeling and simulation tools for predicting the tribological behavior of mixed-elastohydrodynamic lubricated contacts. His current research interests focus on tribological solutions for energy efficiency and sustainability, with emphasis on computational tribology, lubrication and contact mechanics, topography characterization, machine learning in tribology, sliding bearings, internal-combustion engines, and reciprocating hermetic compressors. Profito can be reached by email at fprofito@usp.br.

Xuan Zhang is a postdoctoral researcher at INM: Leibniz Institute for New Materials, Germany. She received her BE and PhD degrees in engineering mechanics from Tsinghua University, in China. Her research interests focus on design and understanding of advanced structures and materials. Her recent work includes design, fabrication, and mechanics of three-dimensional (3D) micro-/nano-architected mechanical metamaterials and nanoporous materials; exploration of the underlying deformation mechanisms of novel nanostructured materials via theory modeling and simulations; and application of 3D mechanical metamaterials to advanced adhesives. Zhang can be reached by email at Xuan.Zhang@leibniz-inm.de.

Karen Ann Thole is a distinguished professor at The Pennsylvania State University where she directs the Steady Thermal Aero Research Turbine (START) Laboratory, focused on advancing aviation sustainability and power generation. Her expertise is in heat transfer and additive manufacturing. She is a Fellow of The American Society of Mechanical Engineers (ASME) and the American Institute of Aeronautics and Astronautics (AIAA). Her awards include the ASME George Westinghouse Gold Medal, the Edwin F. Church Medal, and the Heat Transfer Memorial Award; and the AIAA Air Breathing Propulsion and Thermophysics Awards. Thole can be reached by email at kthole@psu.edu.